



Article

Climate and Management Practices Jointly Control Vegetation Phenology in Native and Introduced Prairie Pastures

Yuting Zhou ^{1,*}, Shengfang Ma ², Pradeep Wagle ³ and Prasanna H. Gowda ⁴¹ Department of Geography, Oklahoma State University, Stillwater, OK 74074, USA² Department of Computer Science, Oklahoma State University, Stillwater, OK 74074, USA; shengfang.ma@okstate.edu³ USDA-ARS, Oklahoma and Central Plains Agricultural Research Center, El Reno, OK 73036, USA; pradeep.wagle@usda.gov⁴ USDA-ARS, Southeast Area, Stoneville, MS 38776, USA; prasanna.gowda@usda.gov

* Correspondence: yuting.zhou@okstate.edu; Tel.: +1-405-744-9168

Abstract: Climate, human disturbances, and management practices jointly control the spatial and temporal patterns of land surface phenology. However, most studies solely focus on analyzing the climatic controls on the inter-annual variability and trends in vegetation phenology. Investigating the main and interacting effects of management practices and climate might be crucial in determining vegetation phenology and productivity. This study examined the impacts of climate and management practices on vegetation phenology and productivity in adjacent native and introduced prairie pastures, which have detailed long-term management records, by combining climate, management, and satellite remote sensing data (e.g., Moderate Resolution Imaging Spectroradiometer (MODIS) and Landsat). Modeled gross primary production (GPP) using vegetation photosynthesis model (VPM) was also included to investigate the dynamics of productivity. When comparing the impacts of the same management practices on different pastures, we used paired comparison, namely, comparing the native and introduced prairies side by side in the same year. The interactions of management practices and climate were investigated through comparing years with similar management but different climate (e.g., years with rainfall or not following baling events) in the same pasture. Results showed that air temperature (T_a) was an important factor in determining the start of the season (SOS) and the length of the season (LOS). Total rainfall (RF) during the annual growing season (AGS, derived from vegetation indices (VIs)) had the largest explanatory power ($R^2 = 0.53$) in explaining the variations in the seasonal sums of VIs. The variations in GPP were better explained by RF ($R^2 = 0.43$) than T_a ($R^2 = 0.14$). Using the thermal growing season (March–October) or AGS climate factors did not show large differences in determining the relationships between phenology, GPP, and climate factors. Drought shortened the LOS and decreased GPP. In terms of management practices, grazing generally reduced the VIs and burning induced early greening-up and enhanced vegetation growth. Drought plus other management practices (e.g., grazing or baling) greatly affected vegetation phenology and suppressed GPP. The negative impacts (i.e., removal of biomass) of grazing on vegetation was compensated by enhanced vegetation growth after good RF. This study demonstrated that the interactions of climate and management practices could be positive (burning plus baling in a good RF year) or negative (grazing/baling plus drought), and can significantly affect vegetation phenology and production.



Citation: Zhou, Y.; Ma, S.; Wagle, P.; Gowda, P.H. Climate and Management Practices Jointly Control Vegetation Phenology in Native and Introduced Prairie Pastures. *Remote Sens.* **2023**, *15*, 2529. <https://doi.org/10.3390/rs15102529>

Academic Editor: Xuanlong Ma

Received: 21 February 2023

Revised: 27 April 2023

Accepted: 6 May 2023

Published: 11 May 2023



Copyright: © 2023 by the authors. Licensee MDPI, Basel, Switzerland. This article is an open access article distributed under the terms and conditions of the Creative Commons Attribution (CC BY) license (<https://creativecommons.org/licenses/by/4.0/>).

Keywords: MODIS; Landsat; interacting effects; gross primary production (GPP); drought; grazing; baling; burning

1. Introduction

Vegetation phenology plays an important role in climate–carbon cycle feedback such as determining the impacts of climate change on the growing season and characterizing the

sensitivity of ecosystem processes to climate change [1–4]. Satellite remote sensing datasets have been extensively used to study vegetation phenology over space and time [5–11]. The Advanced Very High Resolution Radiometer instrument (AVHRR) onboard the National Oceanographic and Atmospheric Administration (NOAA) satellite series had been used to study global-scale phenology back in the 1990s [11]. Other satellite datasets, including the Satellite Pour l’Observation de la Terre-Vegetation (SPOT-VGT) [12], Landsat [13], and the Moderate Resolution Imaging Spectroradiometer (MODIS), have also been utilized to investigate vegetation phenology to understand the impacts of phenological changes on terrestrial carbon budget and evaluate crop productivity and management [14]. Many studies combined two [6,8,15] or more satellite datasets [9,16] to take advantage of different sensors with various spatial and temporal resolutions. For example, one can merge the long-term AVHRR and Landsat datasets with high-quality but short-term MODIS and SPOT-VGT datasets to investigate the trends of regional land surface phenology [16].

The Normalized Difference Vegetation Index (NDVI), which combines two vegetation-sensitive bands to strengthen and simplify the information contained in vegetation [17,18], is the most widely used index in vegetation monitoring. It first gained popularity in vegetation phenology detection [2,19–21]. The Enhanced Vegetation Index (EVI) [22], which reduces sensitivity to soil and atmospheric effects, was frequently used in recent years in the monitoring of vegetation phenology [5,7,23]. Hybrid approaches, which combine multiple indicators, have also been developed [10,12,24]. In terms of phenology detection methods, a large variety of software packages exist [5,7,9,10,25–28], with TIMESAT being one of the most popular software packages to analyze time series of satellite data [28].

Many case studies have tried to investigate the climatic controls on vegetation phenology using climate data and vegetation phenology from various satellite datasets [2,23,29,30]. However, to truly understand carbon cycling on a global scale, assessing the impacts of climate and management interactions on vegetation phenology is also essential, though challenging to quantify due to their confounding effects [9,26,31,32]. Using information on vegetation greenness and land surface temperature from MODIS, a disturbance index named MODIS Global Disturbance Index has been developed to study global disturbances [33,34]. This index can help detect disturbance events, but has difficulty in identifying the causality without the support of other climate and management data. Additionally, the commonly used 500 m surface reflectance product [35] is generally too coarse for monitoring localized disturbances [36] such as grazing, baling, and patch burning. Finer spatial resolution of Landsat imagery (optical: 30–80 m and thermal: 60–120 m) can enable more detailed vegetation monitoring. While in comparison to the daily MODIS overpass, the 16-day revisit cycle of Landsat is more susceptible to cloud cover, making it prone to miss the short-term disturbances and quick recovery of vegetation after disturbances. Combining MODIS and Landsat is a good strategy to balance the trade-off between spatial and temporal resolutions [37] for studying field-scale vegetation responses to climate and management.

In addition to frequent exposure to drought [38–44], grassland in the Great Plains of the United States also experiences various common management practices such as burning, grazing, and baling (hay harvesting). Prescribed burning is a recommended management practice to sustain the grassland ecosystem function and structure [45–47]. Grazing and baling remove the aboveground biomass and thus can reduce canopy coverage and vegetation photosynthesis. The effects of grazing on vegetation vary under different climate conditions and grazing intensity [48]. The interactions of climate and management or multiple management practices in the same year could make their impacts even more complicated to assess [49] due to the many possible combinations of climate and management practices. For example, burning could have a positive or negative effect on grassland phenology and productivity depending on the rainfall of the year. In order to detect the complex/confounding interactions of climate and management, site-specific investigation of vegetation phenology becomes valuable. The repeated observations of satellite imagery provide an opportunity to examine the dynamics of vegetation phenology using time series

data. High-quality climate data and detailed management records help ascribe the causes of variations in vegetation phenology and productivity [48].

This study aims to combine MODIS and Landsat imagery to examine the impacts of climate and management interactions on vegetation phenology and gross primary production (GPP) in native and introduced prairie pastures where detailed management and quality-controlled climate and eddy flux data exist. First, the relationships between vegetation phenology, GPP, and climate factors were examined using MODIS and climate data from a weather station located in the native prairie pasture. The impacts of a single factor (climate or management) on intra-annual dynamics of vegetation phenology were then investigated through combining MODIS and Landsat data. Finally, the impacts of interactions of climate and management on vegetation phenology and GPP were examined. Results from this detailed field-scale study will help ranchers adopt appropriate management strategies based on different climatic conditions.

2. Materials and Methods

2.1. Study Area

The study area is located at the United States Department of Agriculture-Agricultural Research Service (USDA-ARS), Oklahoma and Central Plains Agricultural Research Center (OCPARC) in El Reno, Oklahoma (Figure 1). It consists of two adjoining pastures: (1) a native pasture (NP) with big bluestem (*Andropogon gerardi* Vitman) and little bluestem (*Schizachyrium halapense* (Michx.) Nash.) as the dominant species [50] and (2) an introduced (managed) pasture (IP) dominated by old world bluestem (*Bothriochloa caucasica* C. E. Hubb.) [37]. The Oklahoma Mesonet El Reno weather station is located within the NP, which provides quality-controlled measurements of several meteorological variables, including precipitation, air temperature, solar radiation, soil moisture, and so on [51] (<http://www.Mesonet.org/>, accessed on 30 June 2020). Each field is equipped with an eddy covariance (EC) system to measure CO₂ and H₂O fluxes. Four MODIS pixels with the majority of them overlapped with the study area are presented in Figure 1. In this study, we focus on the two MODIS pixels having EC towers where modeled GPP and EC-derived GPP have already been compared [37,52].

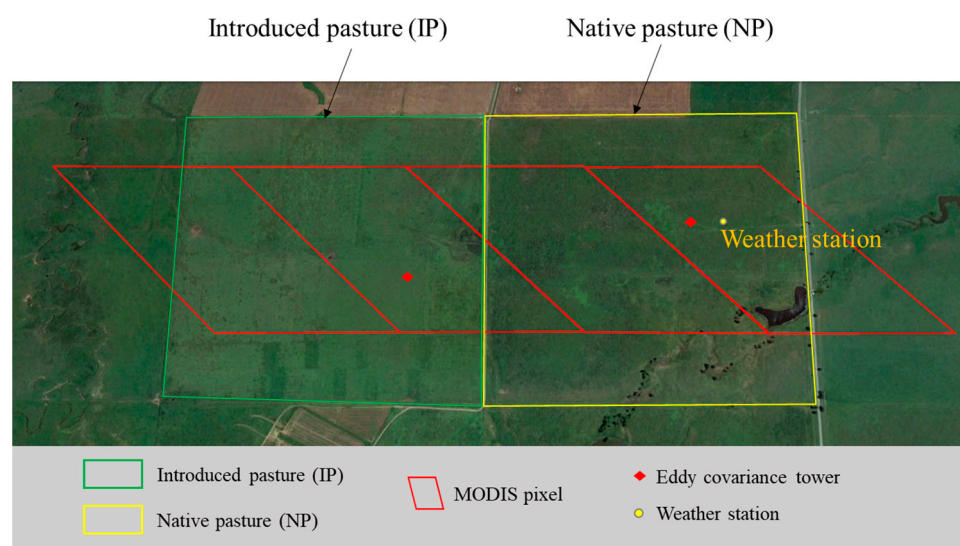


Figure 1. Location of the study area overlapping with MODIS pixels (red lines). Locations of the Oklahoma Mesonet El Reno site (yellow point) and two eddy covariance towers (35.54865° N, 98.03759° W in native pasture and 35.54679° N, 98.04529° W in introduced pasture) are also shown (red diamonds). Yellow rectangle is the boundary of the native pasture and green rectangle is the boundary of the introduced pasture.

2.2. Climate Data

The daily rainfall (RF) and average air temperature (Ta) were collected from the Oklahoma Mesonet El Reno station in the NP. Annual and thermal growing season (AGS and TGS, respectively) total RF and mean Ta were calculated for 2000–2015. The AGS climate metrics were calculated for the entire calendar year (January–December) while TGS climate metrics were calculated specifically for March–October (i.e., growing season) in each year. The ratios between AGS and TGS RF were also calculated to further indicate the rainfall deficit during the growing season each year. Since the weather station is located in the NP and the IP is just beside, we used the same weather data for both pastures.

Total RF varied largely in both AGS and TGS during the study years. Wet years were observed in 2007, 2013, and 2015, while 2001, 2003, 2006, 2011, 2012, and 2014 had less than normal total RF (Figure 2a). Wet and dry years were defined by the mean plus or minus one times of standard deviation. The lowest ratio of TGS to AGS RF (0.64) during the study period was observed in 2011. Average Ta for the TGS in 2006, 2011, and 2012 was more than 1 °C higher than the mean, indicating severe dry and hot years (Figure 2b).

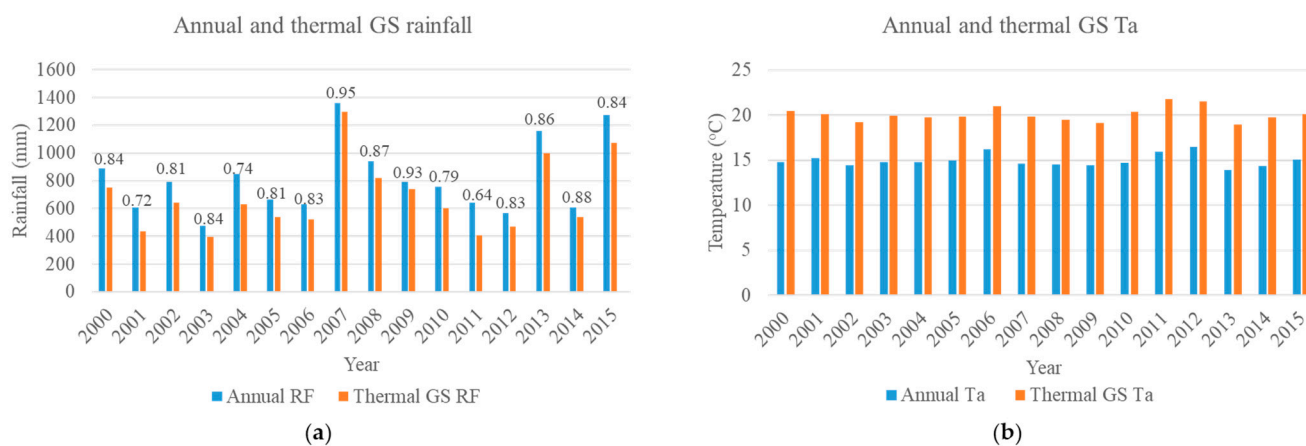


Figure 2. Sum rainfall (a) and average air temperature (b) in annual and thermal growing season. The ratio of thermal growing season to annual growing season rainfall are labeled to further indicate the rainfall deficit in the growing season.

2.3. Management Records for the Native and Introduced Pastures

The USDA-ARS OCPARC has archived long-term management records for the NP and IP. This study only focuses on the years after 2000 when the MODIS time series were available to detect vegetation phenology and model GPP. The major management practices in the NP were grazing and occasionally burning, while the IP was more intensively managed. Only in 2005 and 2006, the NP field was divided into two sub-sections. The northern half of the NP was burned before the 2005 growing season, while the southern half was not burned. Management practices in the IP were much more complex with the occurrence of burning, baling, grazing, weed control, and fertilization occurring in different years. The entire IP field was not homogeneously covered by the old world bluestem until 2009. Perennial rye grass (*Lolium perenne*) subplots existed in the IP field before 2009. Thus, data prior to 2009 were not included for the IP. The major management practices in the NP and IP from 2009 to 2015 are summarized in Table 1.

Table 1. Major management practices in the native pasture (NP) and introduced pasture (IP) from 2009 to 2015.

Year	Native Pasture	Introduced Pasture
2009	(1). Stocking rate 0.39 head/ha for May–October	(1). Burned on 15 April 2009; (2). May~1st, Weed control and fertilization (3). July~1st, Hayed
2010	(1). Stocking rate 0.37 head/ha for May–October	(1). Burned on 18 March 2010; (2). July~1st, Hayed
2011	(1). Stocking rate 0.45 head/ha for May–October	(1). July~1st, Hayed
2012	Rested all year	(1). Stock rate 0.83 hd/ha for January–May and 0.32 hd/ha for June–July
2013	(1). Burned on 3/6/2013; (2). Stocking rate 0.78 head/ha for December	(1). Stock rate of 0.64 hd/ha for January–March
2014	(1). Stocking rate 0.78 head/ha for April, May, July and November	(1). 9 April 2014 Burned; (2). 7/23 60% of East half of pasture cut for hay, 8/15 40% of East half of pasture cut for hay; (3). Stock rate of 0.40 hd/ha for September–December
2015	(1). Stocking rate 0.78 head/ha for February and 0.39 head/ha for June–July	(1). Stock rate of 0.40 hd/ha for January–February and June–July; (2). Stock rate of 0.96 hd/ha for August–December

2.4. MODIS and Landsat Images and Vegetation Indices

The 8-day composite MODIS surface reflectance product (MOD09A1) [35] was used to calculate two commonly used vegetation indices (Vis): NDVI, (Equation (1)) [17,18] and EVI (Equation (2)) [22]. Both NDVI and EVI were then used to derive vegetation phenology metrics and greenness.

$$\text{NDVI} = \frac{\rho_{\text{nir}} - \rho_{\text{red}}}{\rho_{\text{nir}} + \rho_{\text{red}}} \quad (1)$$

$$\text{EVI} = 2.5 \times \frac{\rho_{\text{nir}} - \rho_{\text{red}}}{\rho_{\text{nir}} + 6.0 \times \rho_{\text{red}} - 7.5 \times \rho_{\text{blue}} + 1} \quad (2)$$

Our study area is located in the center of the image tile (Path28/Row35) and was not affected by the strips in Landsat 7 imagery caused by the failure of the ETM+ scan line corrector. Thus, both Landsat 7 and Landsat 8 data were included in the analysis. All of the available Landsat 7 and Landsat 8 surface reflectance products during the study period (2000–2015) covering the study area were downloaded from the USGS EarthExplorer (<http://earthexplorer.usgs.gov/>, accessed on 10 July 2020) and images for the NP and IP were extracted. Only clear pixels were included in data analysis based on the quality assessment band, which helped to exclude image artifacts caused by cloud, cloud shadow, and aerosols [37,53]. The color composite images (shortwave infrared (SWIR-2), near infrared (NIR), and red bands as RGB) were used to reduce atmospheric effects and to highlight vegetation. The Landsat EVI values for the paired and homogeneous subplots were calculated to compare the impacts of management practices on vegetation phenology.

2.5. Vegetation Phenology Metrics and Greenness Derived from MODIS Vegetation Indices

The time series of NDVI and EVI from MODIS were used to estimate phenology metrics from the TIMESAT software package [28]. Major phenology metrics included in this study were the start of season (SOS), end of season (EOS), length of season (LOS), and peak value of NDVI/EVI. The sum and average NDVI/EVI were also calculated corresponding to the SOS and EOS in each year. As mentioned before, the IP did not have

homogeneous land cover type until 2009, thus the phenology metrics and greenness data were only used from 2009 onwards for the IP, while they were used for the entire study period (2000–2015) for the NP.

2.6. Gross Primary Production (GPP) Estimates from the Vegetation Photosynthesis Model

The Vegetation Photosynthesis Model (VPM) [54] was used to estimate GPP from 2000 to 2015 for NP and from 2009 to 2015 for IP. The VPM estimates GPP as a product of light use efficiency (ϵ_g) and absorbed photosynthetically active radiation (APAR) by the chlorophyll ($APAR_{chl}$):

$$GPP_{VPM} = \epsilon_g \times APAR_{chl} \quad (3)$$

$$APAR_{chl} = fPAR_{chl} \times PAR \quad (4)$$

where $fPAR_{chl}$ is set equal to EVI. The ϵ_g is derived by down-regulating the theoretical maximum light use efficiency (ϵ_0) with scalars of temperature (T_{scalar}) and water (W_{scalar}) stresses.

$$\epsilon_g = \epsilon_0 \times T_{scalar} \times W_{scalar} \quad (5)$$

The VPM-estimated GPP has been evaluated using results for the two EC sites located in the NP and IP by previous studies [37,52,55]. The comparison showed good agreement between the two GPP products, indicating the reliability of the modeled GPP for further analysis in this study.

2.7. Statistical Analysis

Using the 16 years of Vis and climate data in NP, we performed regression analyses to examine the relationships between phenology metrics/greenness and climatic variables. Multiple combinations were tested to include possible causal relationships (Table 2). Early and late seasons were defined for March–June and July–October, respectively. Both NDVI- and EVI-derived phenology metrics and greenness were correlated with different climate factors. Since the IP was converted to old world bluestem and had homogeneous land cover type only after 2009, we did not examine the phenology–climate relationships at the IP site. The TGS GPP sums were also correlated with the TGS/AGS total RF and average Ta.

Table 2. Pairs of parameters used in a simple linear correlation for vegetation phenology and greenness. NDVI: normalized difference vegetation index, EVI: enhanced vegetation index, SOS: start of the season, EOS: end of the season, and LOS: length of the season.

SOS (NDVI/EVI-based)	Early season total RF
	Early season average Ta
	Early season maximum Ta
EOS (NDVI/EVI-based)	Late season total RF
	Late season average Ta
LOS (NDVI/EVI-based)	Thermal GS total RF
	Thermal GS average Ta
	Annual GS total RF
	Annual GS average Ta
Peak NDVI/EVI	Early season total RF
	Early season average Ta

Table 2. Cont.

NDVI/EVI sum	Thermal GS total RF
	Thermal GS average Ta
	Annual GS total RF
	Annual GS average Ta
NDVI/EVI average	Thermal GS total RF
	Thermal GS average Ta
	Annual GS total RF
	Annual GS average Ta

3. Results

3.1. Relationships of Vegetation Phenology, Greenness, and GPP with Climate Factors

After analyzing the relationships between phenology metrics/greenness and climate factors, the results with coefficients of determination (R^2) larger than 0.4 were selected and presented in Figure 3. The NDVI- (first column panels in Figure 3a) and EVI-derived (second column panels in Figure 3a) SOS advanced with increasing early season average Ta, demonstrating the role of higher spring temperature for greening-up of vegetation. The NDVI- and EVI-derived LOS was negatively correlated with the TGS and AGS average Ta with a larger R^2 in the former. The relationships between NDVI- or EVI-derived phenology metrics and climate factors were generally similar.

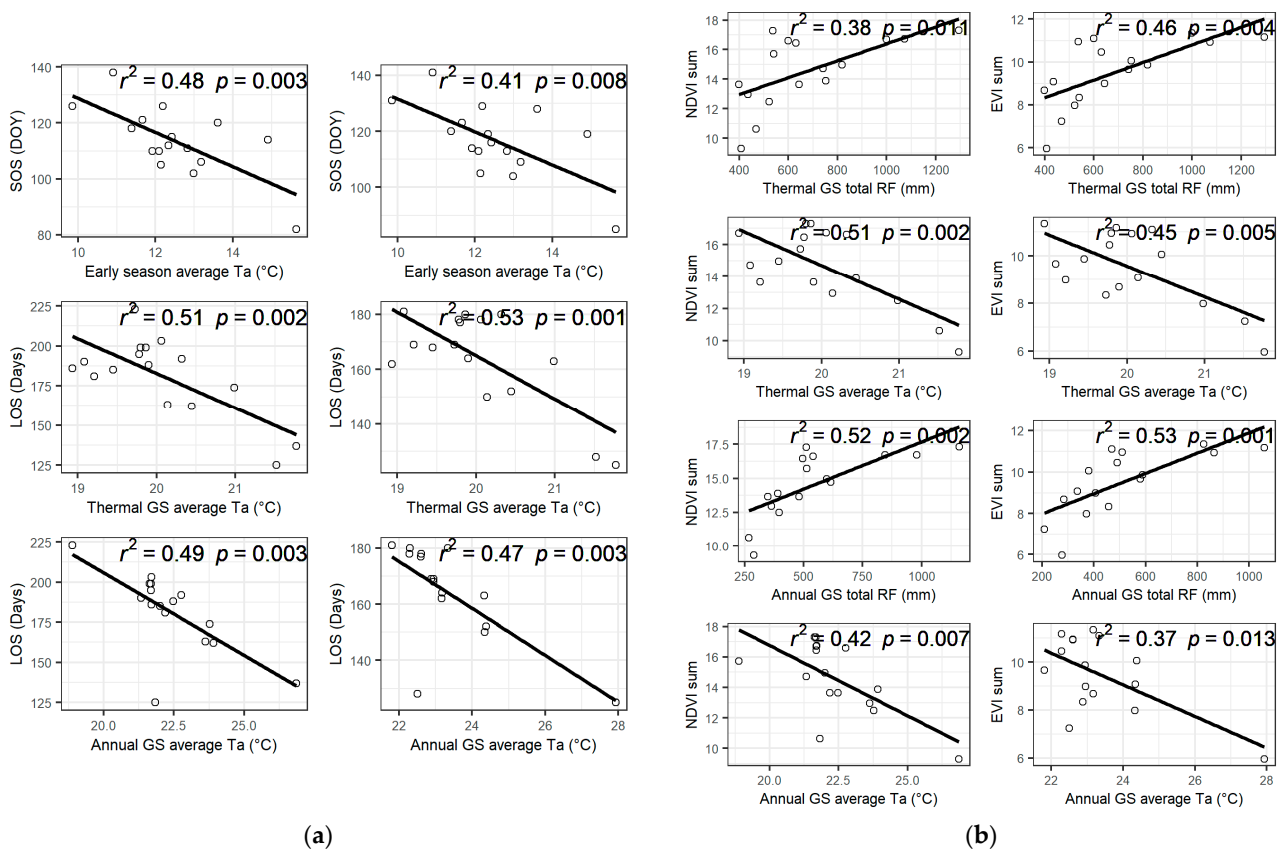


Figure 3. Simple linear regressions with coefficients of determination larger than 0.4 for (a) phenology metrics vs. climate, (b) greenness metrics vs. climate. The first, second, third, and fourth column panels are for NDVI-derived phenology metrics, EVI-derived phenology metrics, NDVI-based greenness, and EVI-based greenness, respectively, in the native pasture.

The NDVI sum was positively correlated with total RF for both TGS and AGS ($R^2 = 0.38$ and 0.52 , respectively), while it was negatively correlated with TGS and AGS average T_a ($R^2 = 0.51$ and 0.42 , respectively) (first column panels in Figure 3b). These relationships indicated that rainfall was a limiting factor while temperature was a stressor, especially during the TGS. The relationships between EVI sum and climate factors also showed similar trends (second column panels in Figure 3b). The VI sum vs. AGS total RF had the largest R^2 values (0.52 for NDVI and 0.53 for EVI), indicating the importance of RF in the influencing of vegetation phenology and productivity.

TGS sum of GPP was positively correlated with total RF during TGS/AGS and negatively correlated with TGS/AGS average T_a (Figure 4). As in the VI vs. climate relationships (Figure 3), RF provided stronger explanatory power than did T_a . GPP showed large variations in both NP and IP (Figure 5). The GPP in 2011 had the lowest values due to severe drought. After IP was homogeneously covered by old world bluestem, GPP in both NP and IP was very similar for the following two years (2009 and 2010). The GPP decreased more in IP than NP during the continuous droughts in 2011 and 2012.

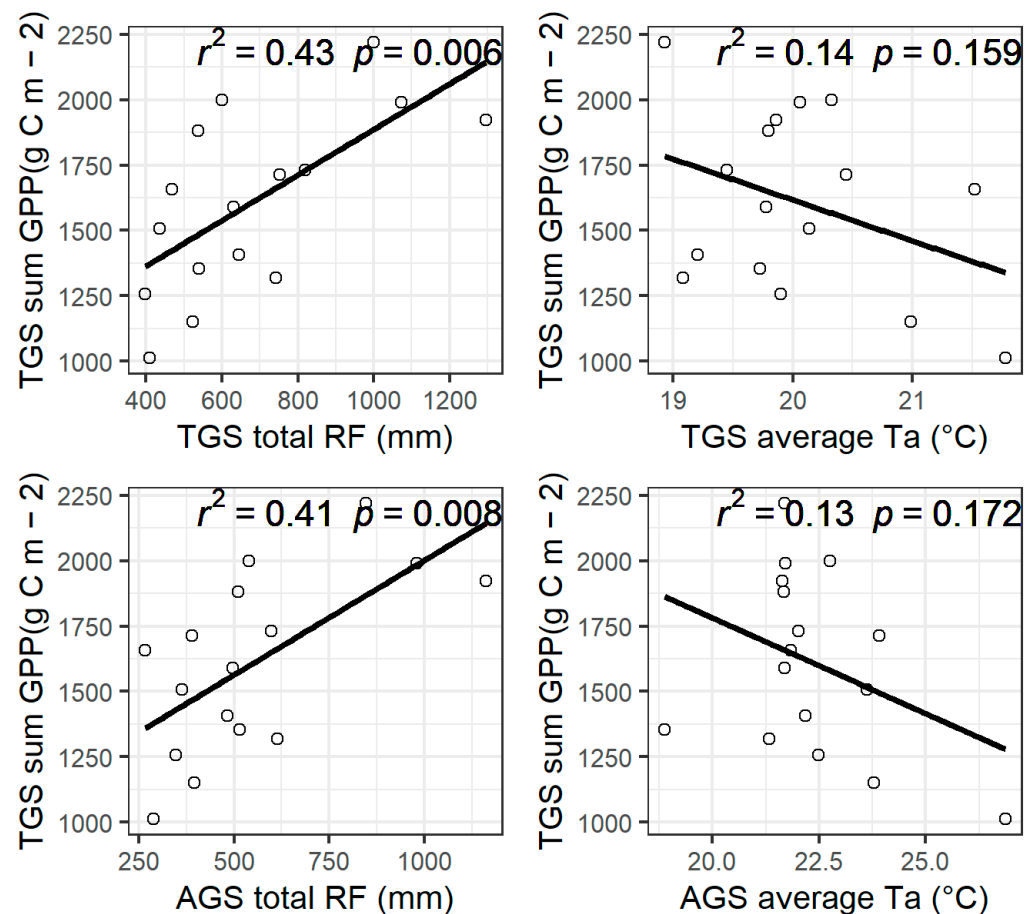


Figure 4. Relationships between thermal growing season sum of gross primary production (GPP) and climate in the native pasture.

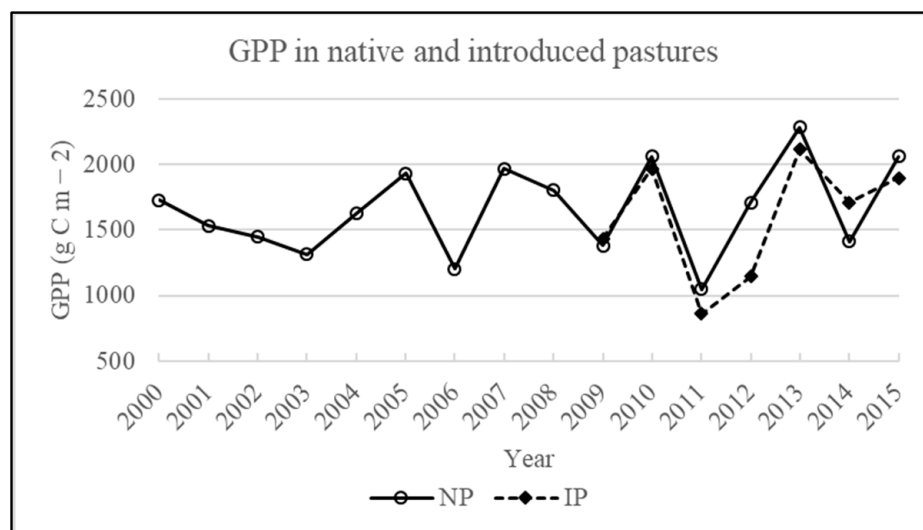


Figure 5. Modeled (using vegetation photosynthesis model) gross primary production (GPP) sums in the native (NP) and introduced (IP) pastures.

3.2. Intra-Annual Dynamics of Vegetation Phenology Affected by a Single Factor

The previous section demonstrated the impacts of total RF and average T_a on vegetation phenology, greenness, and GPP using annual data. However, the relationships were not very strong, necessitating the analysis of intra-annual dynamics of vegetation phenology. This section analyzed the impacts of a single climate event (drought) or management practice (grazing and burning) on vegetation phenology in specific years.

3.2.1. Impacts of Drought in the NP

Both 2006 and 2012 were drought years (Figure 2). Since the IP field was not homogeneous in 2006, we investigated the impacts of drought in the NP only. Vegetation in the NP greened up earlier in 2012 (Figure 6, left panel, right side) than in 2006 (Figure 6, middle panel, right side) due to a warmer and wetter spring (15.64 °C and 28.78 mm for 2012; 14.91 °C and 26.24 mm for 2006). Additionally, the VIs in 2012 recorded much higher values than in 2006 especially during the early growing season (Figure 6, right panel). However, the plants quickly exhausted soil moisture because of the combination of early season rapid growth and subsequent precipitation deficit and high temperature in the summer of 2012. These circumstances caused a so-called “flash drought [44,56]”, where vegetation became dormant after the flash drought and resulted in the left-skewed VIs curves in 2012.

3.2.2. Impacts of Grazing in the NP and IP

In 2009, IP was not grazed and NP was grazed from May through October by breed cows (635 kg average weight) at a stocking rate of 0.41 head/ha. The two pastures were visually similar on DOY 167 (mid-June) (Figure 7, left panel) in 2009. With continuous grazing pressure, NP became less green than the IP. In 2015, IP was grazed throughout most of the year, while NP was grazed for only three months (February, June, and July). However, the two pastures did not show much difference in greenness during the 2015 growing season (Figure 7, right panel). When we overlay RF with VIs for these two years (Figure 8), the interactions of RF patterns and grazing were clear. In 2015, RF was greater than in 2009 and the majority of RF was received during peak growth (May and June). In 2009, the majority of RF came later in the growing season (August through mid-October). Thus, the VIs values in 2015 were higher and the sites showed sustained growth over the entire growing season. However, in 2009, the lack of early season rain and lower overall RF prevented the recovery growth in grazed pasture.

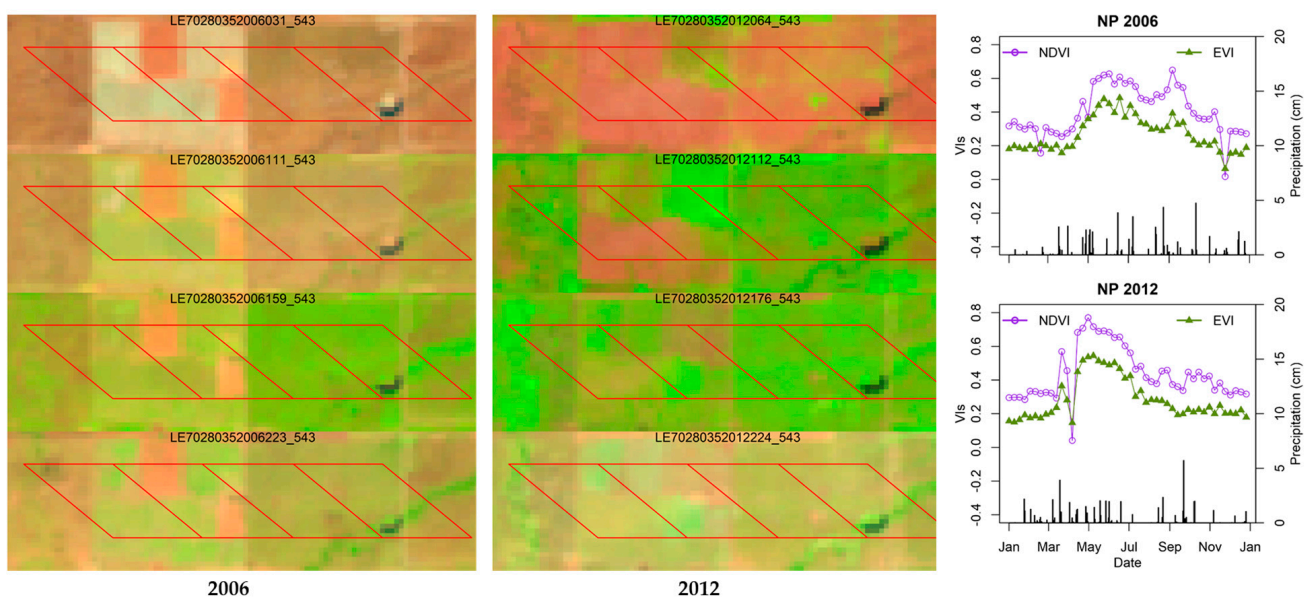


Figure 6. Drought in the native (NP) and introduced (IP) pastures in 2006 and 2012. The left panels are Landsat color composite (SWIR-2, NIR, and Red) images overlapped with the MODIS in 2006 (images for DOY 31, 111, 159, and 223, top to bottom, respectively). The middle panels are for 2012 (images are for DOY 64, 112, 176, and 224, top to bottom, respectively). The right panels are NDVI and EVI time series for the NP in 2006 and 2012 from the MODIS. Daily RF are also added in the VIs plots to show the RF deficit.

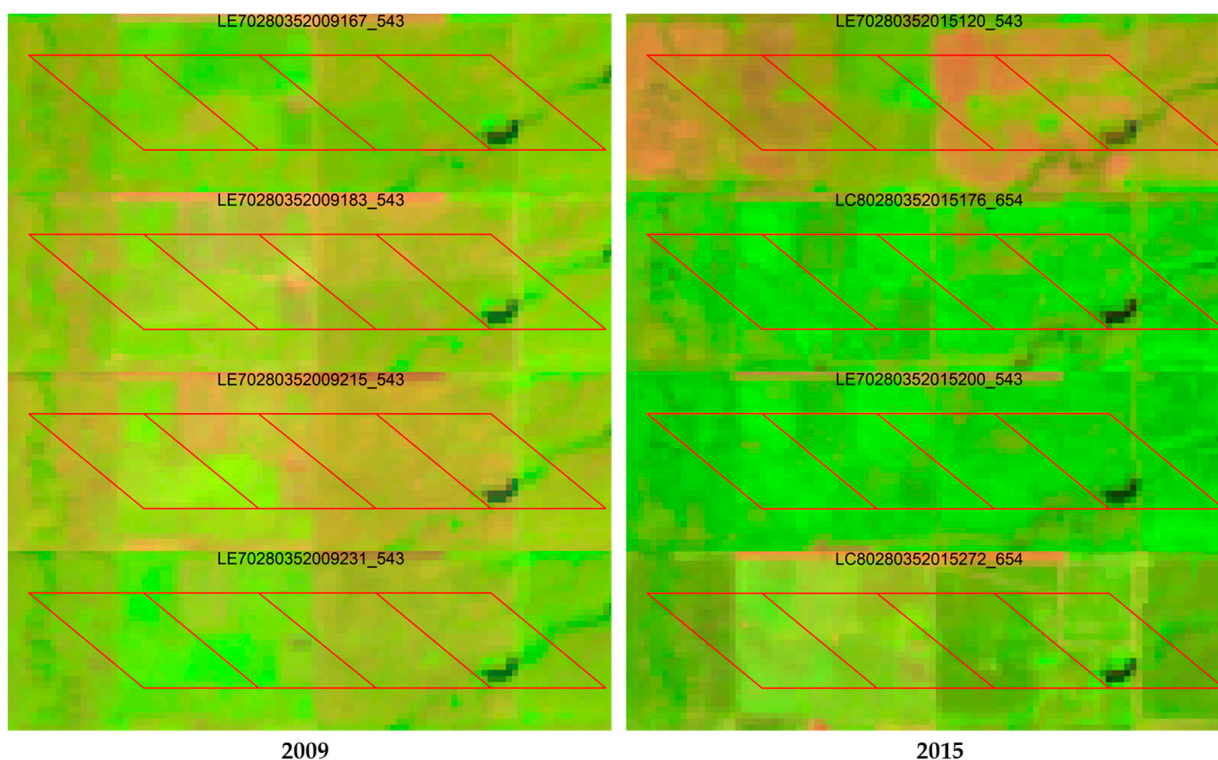


Figure 7. The impacts of grazing on vegetation phenology reflected by color composited Landsat images (Band combination is the same as in Figure 6). The left panels are for 2009 (images are for DOY 167, 183, 215, and 231, top to bottom, respectively) and the right panels are for 2015 (images are for DOY 120, 176, 200, and 272, top to bottom, respectively).

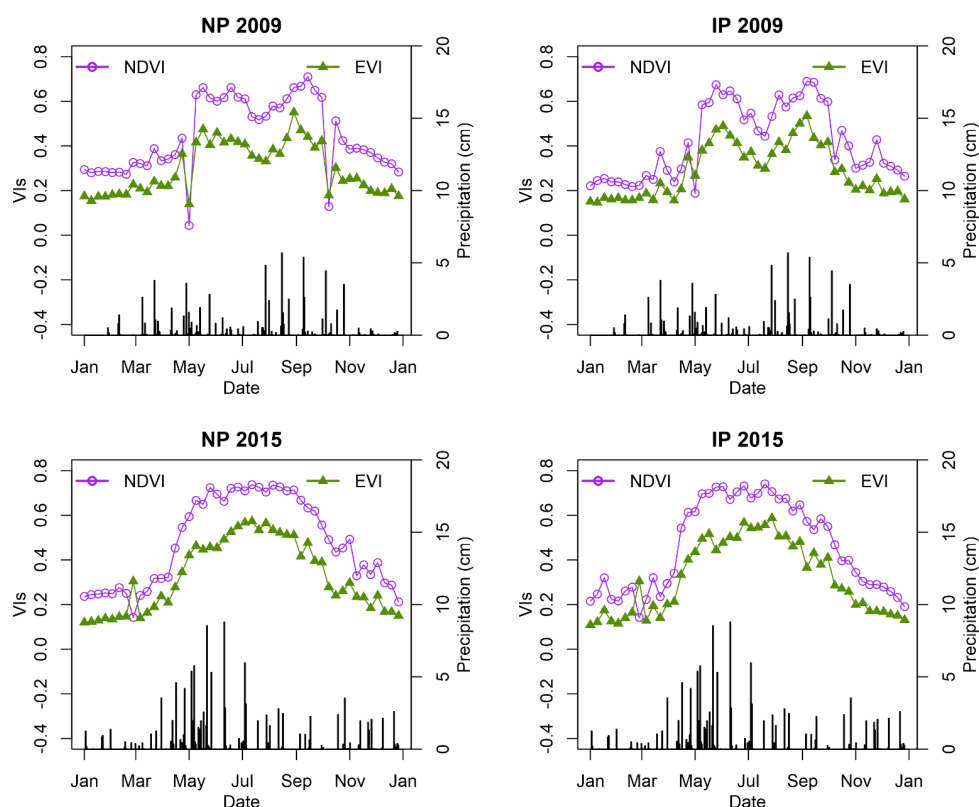


Figure 8. The time series of NDVI and EVI from MODIS in 2009 and 2015 for the native (NP, **left**) and introduced (IP, **right**) pastures. The top panels are 2009 and the bottom panels are 2015.

3.2.3. Impacts of Burning in the NP and IP

The northern half of the NP was burned in 2005 and the entire area was burned in 2013 (Figure 9). Burning caused early greening-up and enhanced vegetation growth in both 2005 and 2013 (Figure 9, left and middle panels). Given the improved vegetation growth caused by burning, VIs were significantly higher in NP than in IP in 2005 and 2013 (Figure 9, right panel; AGS NDVI is 0.625 in NP and 0.592 in IP). However, this might have been attributed to the differences in species composition between NP and IP. We, therefore, extracted a pair of subplots within burned and non-burned areas of NP and analyzed the EVI values from Landsat images from 2005 to evaluate the impact of burning on the same species (native tallgrass). Burning (8 March 2005, DOY67) initially decreased EVI values compared to non-burned (Figure 10), but the EVI values were much higher in the burned subplot than in the unburned subplot during the entire growing season, demonstrating that the burning enhanced vegetation growth.

3.3. Impacts of Climate and Management Interactions on Vegetation Phenology and GPP

3.3.1. Interactions of Burning plus Baling with RF in the IP

The IP was burned in both 2010 and 2014 while part of it was also baled for hay (Table 1). Time series Landsat images captured the burning and baling events in both years well (Figure 11, left and middle panels). The two baling events which occurred during different periods in 2014 were also captured (Figure 11, third and fourth figures in the middle panel). As expected (Section 3.2.3), the two burning events enhanced vegetation growth, making the land surface greener in IP than in unburned NP. To investigate the interactions of burning and baling, we generated the paired subplots of burning only and burning plus baling, and then analyzed EVI values for the paired plots in 2010 and 2014 from high-quality Landsat surface reflectance data.

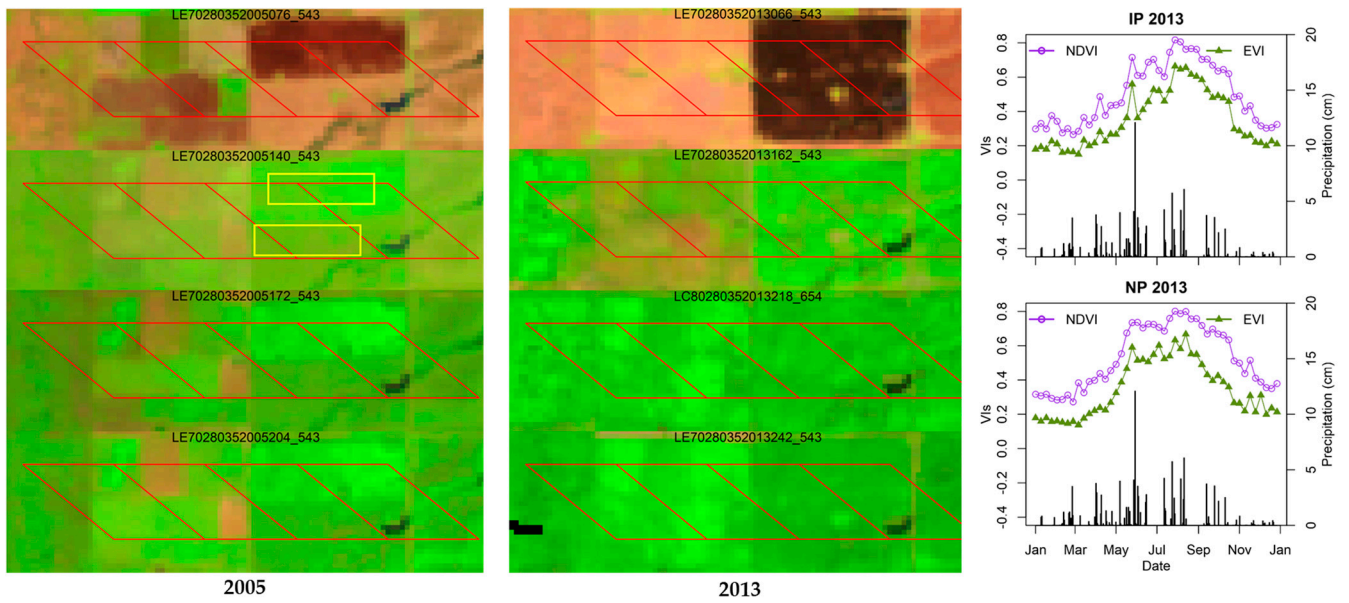


Figure 9. The impacts of burning on vegetation phenology reflected by color composed Landsat images and time series of NDVI and EVI from the MODIS. The left panels are Landsat color composite images for 2005. The middle panels are for 2013. The right panels are NDVI and EVI time series for the introduced pasture (IP, (top)) and native pasture (NP, (bottom)) in 2013 from the MODIS. Yellow boxes in the second figure of the left panels are the subplots used in further analysis using Landsat imagery.

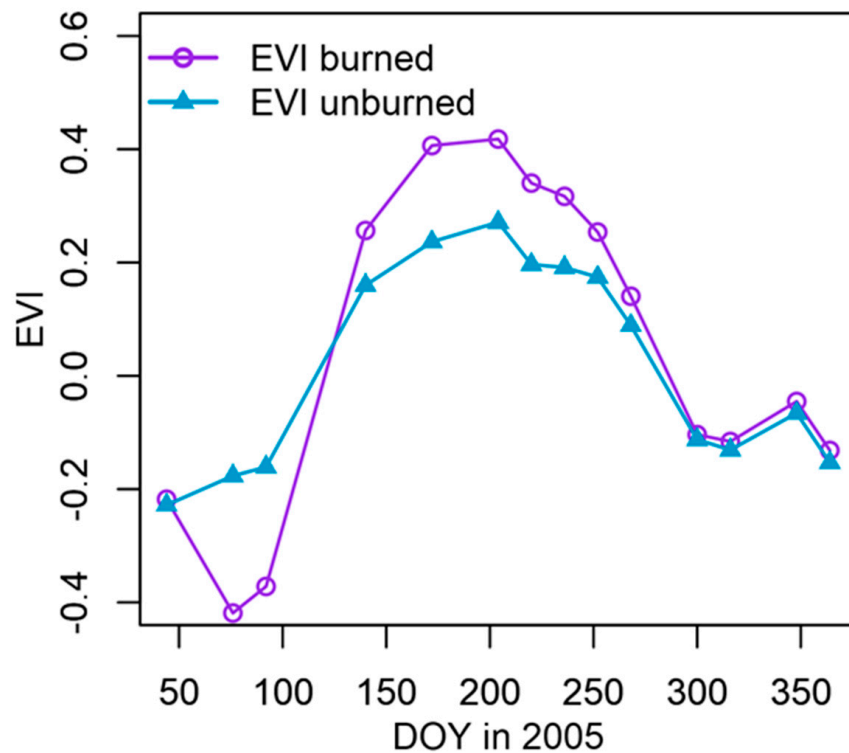


Figure 10. Comparison between burned and unburned subplots in the native pasture in 2005 using EVI from Landsat.

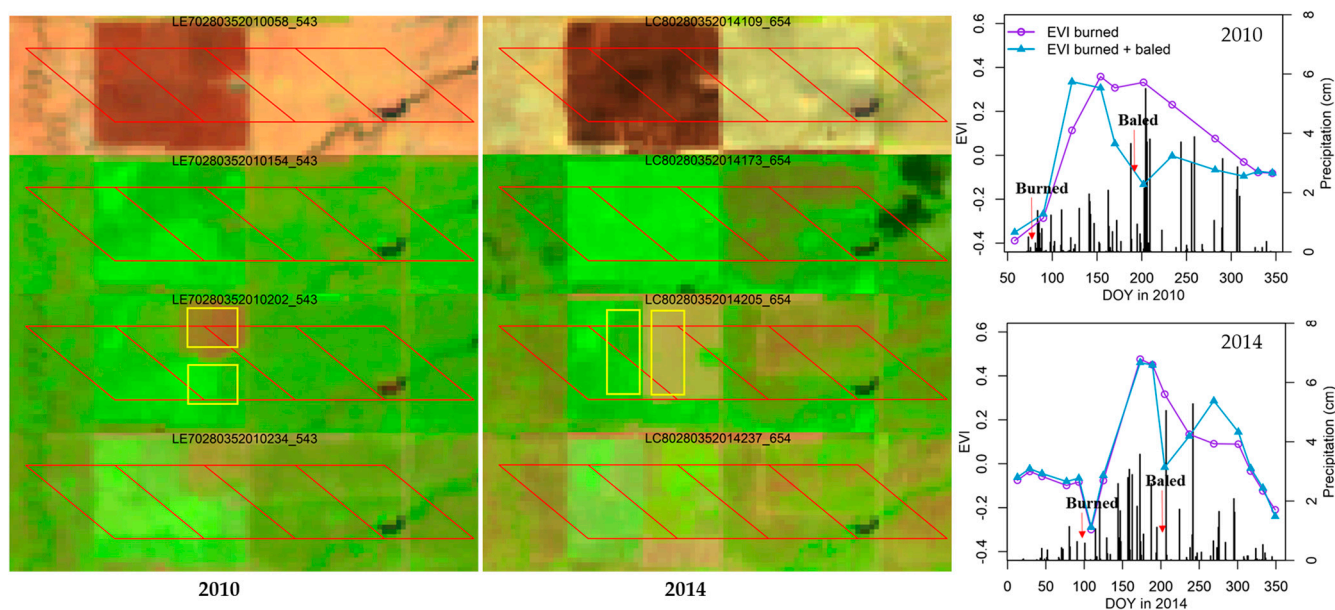


Figure 11. Interactions of burning plus baling with rainfall (RF) in the introduced pasture (IP) in 2010 ((left) panels) and 2014 ((middle) panels), and the Landsat-based EVI values for the paired subplots of burning only and burning plus baling ((right) panels). Yellow rectangles are the subplots used to extract EVI values. Daily RF data were also marked out in the time series EVI values.

The vegetation regrowth after baling can be observed from the EVI values in both 2010 and 2014 (Figure 11, right panel). However, the extent of vegetation regrowth was different. The burned and burned plus baled subplots had very similar EVI values before the baling in 2014. The baling immediately decreased EVI. Then, the EVI values in the burned plus baled subplot surpassed the burned-only subplot due to the removal of senesced plant material and quick vegetation regrowth. We can also see the vegetation regrowth after baling in 2010 but the extent of increasing in EVI was much less compared to 2014. The precipitation deficit after baling in 2010 (13 July–23 August accumulated RF was 0.9 cm) suppressed the vegetation regrowth. In contrast, there were large amounts of precipitation after baling in 2014 (27 July–6 September accumulated RF was 13.7 cm), which greatly facilitated the vegetation regrowth.

3.3.2. Drought plus Grazing in the NP and Drought plus Baling in the IP

In 2011, NP was affected by drought plus grazing and IP was affected by drought plus baling. The vegetation phenology was very similar in the two pastures despite different management practices (Figure 12). Drought shortened the LOS through advancing the EOS. Both pastures had increased VIs after relatively concentrated precipitation in August. Although there was a large rain event in early November (a typical time for the first frost in the study area), it was not effective for vegetation growth due to vegetation senescence and low temperature.

3.3.3. Summary of Vegetation Phenology and GPP under Different Climate and Management

The major phenology metrics, greenness, and GPP in both NP and IP from 2009 (the year with homogeneous land cover in IP) to 2015 are summarized in Table 3. Drought in 2011 and 2012, combined with other management practices, greatly shortened the LOS (an average of 47 days). Both the NP and IP had the largest GS EVI average and sum in 2013 because of the large amount of rainfall in the AGS. Although annual GPP appears to be correlated with the AGS RF, it is clear that other factors play a major role as well. Burning and high AGS RF caused the highest production in 2013 at the NP. It was in the same year that IP, which had no other types of management, had the highest GPP. Grazing decreased

GPP at the IP when compared to the IP in 2013 and 2015. The interactions of drought and other management practices (grazing or baling) greatly suppressed GPP in both NP and IP. The impacts of burning plus baling combinations increased the vegetation production in good rainfall years such as 2014.

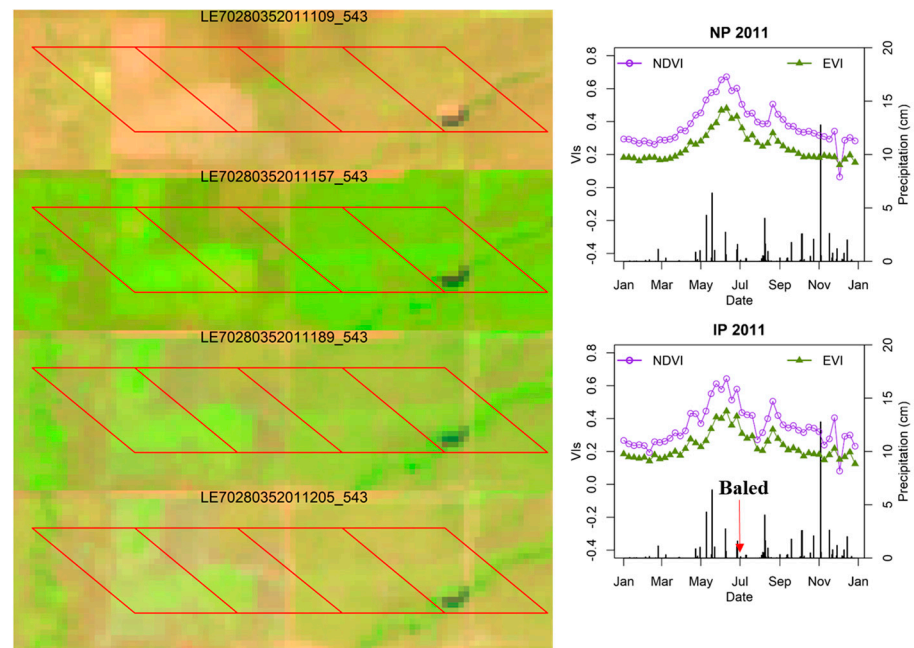


Figure 12. Impacts of drought plus grazing in the native pasture (NP) and drought plus baling in the introduced pasture (IP). The (left) panels are color composite Landsat images. The (right) panels are NDVI and EVI for the NP and IP from the MODIS. Daily rainfall (RF) data were also marked out.

Table 3. Summary of phenology metrics, greenness, and gross primary production (GPP) in the native pasture (NP) and introduced pasture (IP) from 2009 to 2015.

Year	Disturbance Type	Pastures	SOS (DOY)	EOS (DOY)	LOS (Days)	GS EVI Average	GS EVI Sum	GPP (g C m ⁻²)	AGS Rainfall (cm)
2015	Three month grazing	NP	113	290	178	0.48	10.92	2062.18	86.56
	Whole year grazing	IP	110	293	182	0.47	11.36	1895.86	
2014	Four month grazing	NP	141	310	169	0.38	8.35	1411.02	45.80
	Burning + baling	IP	133	282	149	0.48	9.16	1711.64	
2013	Burning	NP	131	294	162	0.52	11.35	2281.61	82.55
	None	IP	137	304	167	0.52	11.49	2111.77	
2012	Drought	NP	85	212	128	0.45	7.24	1709.79	20.80
	Drought + grazing	IP	93	209	116	0.41	6.10	1143.39	
2011	Drought + grazing	NP	128	253	125	0.35	5.95	1049.30	27.71
	Drought + baling	IP	131	257	126	0.33	5.59	863.00	
2010	Six month grazing	NP	114	293	180	0.46	11.09	2059.05	47.00
	Burning + baling	IP	110	291	181	0.51	11.66	1965.43	
2009	Six month grazing	NP	116	297	181	0.40	9.66	1382.18	57.91
	Burning + baling	IP	128	296	168	0.41	9.09	1435.70	
2006	Drought	NP	119	282	163	0.38	7.98	1204.27	37.11

Note: the LOS might not equal to the differences between EOS and SOS due to different rounding.

4. Discussion

4.1. Combination of MODIS and Landsat to Study Vegetation Phenology and Production

Results showed that grassland phenology and production were jointly controlled by climate and management practices. The management practices such as burning, grazing, and baling examined in this study can be considered anthropogenic disturbances on vegetation. The climate- and human-induced disturbances on vegetation have different spatial and temporal extents with various severity. For example, long-term and short-term flash droughts can exert different influences on vegetation phenology and production [44,56]. Additionally, the baling-affected area and grazing intensity can be different among fields [37,57,58]. To balance the consideration of spatial and temporal resolutions in studying vegetation phenology and production, the combination of coarser spatial resolution but higher temporal resolution datasets (i.e., MODIS) and finer spatial resolution but lower temporal resolution datasets (i.e., Landsat) becomes necessary and straightforward. These types of combinations can be used to better characterize regional and localized disturbances on vegetation.

Utilizing the higher temporal resolution of MODIS and higher spatial resolution of Landsat enables the characterization of inter- and intra-annual variations of vegetation phenology and production. More importantly, it can help ascribe the causes of variations in vegetation phenology and production with the auxiliary climate data and management records, which provides more ecological understanding of those disturbances [59,60] and more possibility to extrapolate to a larger scale. The ever-increasing remote sensing data volumes and computational methods have enabled the wide application of different satellite datasets to study vegetation dynamics. The Google Earth Engine, which contains many global satellite datasets including MODIS and Landsat, has led to rapid advances in land cover and land use change, disturbances detection, and regional modeling [61–63]. Using this free and powerful platform, one can study both the global and localized vegetation phenology and production through combining different satellite datasets, such as MODIS and Landsat.

4.2. The Impacts of Climate and Management Interactions on Vegetation Phenology and GPP

Both climate and management can affect vegetation phenology and GPP. To achieve higher production, ranchers use different management strategies in grasslands which makes the interactions of climate and management an important aspect in determining grassland phenology and GPP. Our results showed that drought itself can shorten the LOS and thus reduce vegetation production (e.g., 2006). However, the interactions of drought and management practices (baling or grazing in 2012) further exacerbated the vegetation conditions. On the positive side, the burning plus baling could be a good management strategy in years with good RF (e.g., 2014) to increase production. Burning can enhance both above- and below-ground plant productivity in tallgrass prairie in good RF years because of more plant-available nitrogen [48]. On the negative side, burning further reduces the availability of soil water and adversely affects forage production in drought years. The impact of cattle grazing is visible during drought but the removal of biomass by grazing is compensated by quick recovery under good RF (Figures 7 and 8). These results suggest that the interactions of climate and management practices are important in determining grassland phenology and productivity.

Previous studies have shown that moisture stress (precipitation deficit) was a dominating factor in controlling the carbon exchange of the prairie [64,65]. This study further demonstrated that the interactions of climate and management practices also played an essential role in controlling grassland phenology and production. However, we did not see the interactions between burning and drought as burning usually occurred in normal to good precipitation years in the study period. The interactions between them are important as the reduced soil moisture and increased temperature and solar radiation at the soil surface due to burning can exacerbate drought conditions and greatly reduce grassland production during dry years [48,66].

4.3. Implications and Future Steps

This study combined MODIS and Landsat imagery to examine the impacts of climate and management interactions on grassland phenology and productivity. The method can be utilized to study field-scale management and climate impacts in other regions. With the auxiliary climate data and management records, assessment of the impacts of specific climate events (e.g., drought) and management (e.g., burning, grazing, or baling) on grassland phenology and productivity can be accomplished. It also allows for inspection of the interactions of climate and management. Combining MODIS and Landsat imagery to study localized disturbances on vegetation can offer new insights for the understanding of the extent, type, and consequences of disturbances.

Intensively managed grassland (both native prairie and introduced pasture) is a major forage source for beef cattle in the region. Thus, higher productivity in grasslands is of great importance to the beef industry. By utilizing satellite data, climate data, and management records, this study demonstrated that the interactions of climate and management can significantly affect forage productivity. Ranchers should consider both management and climate when trying to maximize forage productivity. The drought plus management in the same year caused the lowest production (Table 3), which indicates the necessity of drought preparedness. Adjusting management strategies by considering climate conditions is a better practice than a static or predefined management plan [67].

As demonstrated in the results, the interactions of climate and management are intricate and dynamic. Further observations over a longer period are necessary to develop effective strategies for forage production in different scenarios. Multisite analysis, such as using data from FLUXNET and AmeriFlux [68], can help understand the interactions in a large geographic domain and potentially produce more general discoveries. MODIS-derived NDVI and EVI were used to calculate phenological metrics. The mixed pixel problem could affect the accuracy of the phenology metrics. Ground observations such as in situ PhenoCam digital images can be used to evaluate them. Moreover, one can fuse the Landsat and Sentinel-2 data to reduce the impacts of the mixed pixel problem. However, the interactions of climate and management could happen fast (e.g., rapid green-up after burning and rainfall). Evening fusing of two optical sensors might miss the critical detecting window [69].

5. Conclusions

By combining MODIS and Landsat imagery, this study examined the impacts of climate and management interactions on vegetation phenology and GPP in native and introduced prairie pastures. Climate factors, namely T_a and RF, played an important role in controlling the SOS/LOS and VIs sum, respectively. GPP was controlled by RF more than T_a . However, the explanatory power was usually low (mostly $R^2 < 0.5$). In general, drought shortened the LOS and decreased GPP, grazing reduced VIs, and burning caused early greening-up and enhanced vegetation growth. The interactions of climate and management practices were evident in specific years only (2011 and 2014). The interactions of drought and management (baling or grazing) can greatly affect vegetation phenology and suppress production. Burning plus baling might be a good management strategy in a good RF year to increase forage productivity. Similar analyses can be adapted in other regions to investigate localized management and climate impacts on vegetation dynamics. The impacts of climate and management interactions suggested that ranchers need to adjust management strategies (dynamic instead of static management plans) based on climatic conditions to maintain productive and sustainable grasslands.

Author Contributions: Conceptualization, Y.Z., S.M., P.W. and P.H.G.; methodology, Y.Z. and S.M.; software, Y.Z. and S.M.; validation, Y.Z., S.M. and P.W.; formal analysis, Y.Z. and P.W.; investigation, Y.Z. and S.M.; resources, P.H.G.; data curation, Y.Z.; writing—original draft preparation, Y.Z.; writing—review and editing, Y.Z., S.M., P.W. and P.H.G.; visualization, Y.Z. and S.M.; supervision, P.H.G.; project administration, P.H.G.; funding acquisition, Y.Z. All authors have read and agreed to the published version of the manuscript.

Funding: This study was supported in part by research grants from the National Science Foundation (NSF) EPSCoR (OIA-1946093), the U.S. Geological Survey under Grant/Cooperative Agreement No. G18AP00077, and the USDA-ARS Office of National Program (Project number: 3070-21610-003-00D).

Data Availability Statement: The code and data used in this work are available from the corresponding author upon reasonable request.

Conflicts of Interest: The authors declare no conflict of interest.

References

1. Menzel, A. Phenology: Its importance to the global change community. *Clim. Chang.* **2002**, *54*, 379–385. [[CrossRef](#)]
2. White, M.A.; Thornton, P.E.; Running, S.W. A continental phenology model for monitoring vegetation responses to interannual climatic variability. *Glob. Biogeochem. Cycles* **1997**, *11*, 217–234. [[CrossRef](#)]
3. Cao, M.; Woodward, F.I. Dynamic responses of terrestrial ecosystem carbon cycling to global climate change. *Nature* **1998**, *393*, 249–252. [[CrossRef](#)]
4. Peñuelas, J.; Filella, I. Responses to a warming world. *Science* **2001**, *294*, 793–795. [[CrossRef](#)]
5. Zhang, X.; Friedl, M.A.; Schaaf, C.B. Global vegetation phenology from Moderate Resolution Imaging Spectroradiometer (MODIS): Evaluation of global patterns and comparison with in situ measurements. *J. Geophys. Res. Biogeosci.* **2006**, *111*, G04017. [[CrossRef](#)]
6. Fisher, J.I.; Mustard, J.F. Cross-scalar satellite phenology from ground, Landsat, and MODIS data. *Remote Sens. Environ.* **2007**, *109*, 261–273. [[CrossRef](#)]
7. Ganguly, S.; Friedl, M.A.; Tan, B.; Zhang, X.; Verma, M. Land surface phenology from MODIS: Characterization of the Collection 5 global land cover dynamics product. *Remote Sens. Environ.* **2010**, *114*, 1805–1816. [[CrossRef](#)]
8. Walker, J.J.; de Beurs, K.M.; Wynne, R.H.; Gao, F. Evaluation of Landsat and MODIS data fusion products for analysis of dryland forest phenology. *Remote Sens. Environ.* **2012**, *117*, 381–393. [[CrossRef](#)]
9. Forkel, M.; Migliavacca, M.; Thonicke, K.; Reichstein, M.; Schaphoff, S.; Weber, U.; Carvalhais, N. Codominant water control on global interannual variability and trends in land surface phenology and greenness. *Glob. Chang. Biol.* **2015**, *21*, 3414–3435. [[CrossRef](#)]
10. Zeng, L.; Wardlow, B.D.; Wang, R.; Shan, J.; Tadesse, T.; Hayes, M.J.; Li, D. A hybrid approach for detecting corn and soybean phenology with time-series MODIS data. *Remote Sens. Environ.* **2016**, *181*, 237–250. [[CrossRef](#)]
11. Moulin, S.; Kergoat, L.; Viovy, N.; Dedieu, G. Global-scale assessment of vegetation phenology using NOAA/AVHRR satellite measurements. *J. Clim.* **1997**, *10*, 1154–1170. [[CrossRef](#)]
12. Delbart, N.; Kergoat, L.; Le Toan, T.; Lhermitte, J.; Picard, G. Determination of phenological dates in boreal regions using normalized difference water index. *Remote Sens. Environ.* **2005**, *97*, 26–38. [[CrossRef](#)]
13. Fisher, J.I.; Mustard, J.F.; Vadeboncoeur, M.A. Green leaf phenology at Landsat resolution: Scaling from the field to the satellite. *Remote Sens. Environ.* **2006**, *100*, 265–279. [[CrossRef](#)]
14. Sakamoto, T.; Yokozawa, M.; Toritani, H.; Shibayama, M.; Ishitsuka, N.; Ohno, H. A crop phenology detection method using time-series MODIS data. *Remote Sens. Environ.* **2005**, *96*, 366–374. [[CrossRef](#)]
15. Atzberger, C.; Klisch, A.; Mattiuzzi, M.; Vuolo, F. Phenological metrics derived over the European continent from NDVI3g data and MODIS time series. *Remote Sens.* **2014**, *6*, 257–284. [[CrossRef](#)]
16. Zhang, G.; Zhang, Y.; Dong, J.; Xiao, X. Green-up dates in the Tibetan Plateau have continuously advanced from 1982 to 2011. *Proc. Natl. Acad. Sci. USA* **2013**, *110*, 4309–4314. [[CrossRef](#)]
17. Rouse, J.W., Jr.; Haas, R.; Schell, J.; Deering, D. Monitoring vegetation systems in the great plains with erts. *NASA Spec. Publ.* **1974**, *351*, 309.
18. Tucker, C.J. Red and photographic infrared linear combinations for monitoring vegetation. *Remote Sens. Environ.* **1979**, *8*, 127–150. [[CrossRef](#)]
19. Wang, J.; Price, K.P.; Rich, P.M. Spatial patterns of NDVI in response to precipitation and temperature in the central Great Plains. *Int. J. Remote Sens.* **2001**, *22*, 3827–3844. [[CrossRef](#)]
20. Pettorelli, N.; Vik, J.O.; Mysterud, A.; Gaillard, J.-M.; Tucker, C.J.; Stenseth, N.C. Using the satellite-derived NDVI to assess ecological responses to environmental change. *Trends Ecol. Evol.* **2005**, *20*, 503–510. [[CrossRef](#)]
21. Massey, R.; Sankey, T.T.; Congalton, R.G.; Yadav, K.; Thenkabail, P.S.; Ozdogan, M.; Sánchez Meador, A.J. MODIS phenology-derived, multi-year distribution of conterminous U.S. crop types. *Remote Sens. Environ.* **2017**, *198*, 490–503. [[CrossRef](#)]
22. Huete, A.; Didan, K.; Miura, T.; Rodriguez, E.P.; Gao, X.; Ferreira, L.G. Overview of the radiometric and biophysical performance of the MODIS vegetation indices. *Remote Sens. Environ.* **2002**, *83*, 195–213. [[CrossRef](#)]
23. Zhang, X.; Friedl, M.A.; Schaaf, C.B.; Strahler, A.H.; Liu, Z. Monitoring the response of vegetation phenology to precipitation in Africa by coupling MODIS and TRMM instruments. *J. Geophys. Res. Atmos.* **2005**, *110*, D12103. [[CrossRef](#)]
24. Liu, Y.; Wu, C.; Peng, D.; Xu, S.; Gonsamo, A.; Jassal, R.S.; Altaf Arain, M.; Lu, L.; Fang, B.; Chen, J.M. Improved modeling of land surface phenology using MODIS land surface reflectance and temperature at evergreen needleleaf forests of central North America. *Remote Sens. Environ.* **2016**, *176*, 152–162. [[CrossRef](#)]

25. Hird, J.N.; McDermid, G.J. Noise reduction of NDVI time series: An empirical comparison of selected techniques. *Remote Sens. Environ.* **2009**, *113*, 248–258. [[CrossRef](#)]
26. Verbesselt, J.; Hyndman, R.; Zeileis, A.; Culvenor, D. Phenological change detection while accounting for abrupt and gradual trends in satellite image time series. *Remote Sens. Environ.* **2010**, *114*, 2970–2980. [[CrossRef](#)]
27. Tan, B.; Morisette, J.T.; Wolfe, R.E.; Gao, F.; Ederer, G.A.; Nightingale, J.; Pedelty, J.A. An Enhanced TIMESAT Algorithm for Estimating Vegetation Phenology Metrics From MODIS Data. *IEEE J. Sel. Top. Appl. Earth Obs. Remote Sens.* **2011**, *4*, 361–371. [[CrossRef](#)]
28. Jönsson, P.; Eklundh, L. TIMESAT—A program for analyzing time-series of satellite sensor data. *Comput. Geosci.* **2004**, *30*, 833–845. [[CrossRef](#)]
29. Julien, Y.; Sobrino, J. Global land surface phenology trends from GIMMS database. *Int. J. Remote Sens.* **2009**, *30*, 3495–3513. [[CrossRef](#)]
30. Keenan, T.F.; Gray, J.; Friedl, M.A.; Toomey, M.; Bohrer, G.; Hollinger, D.Y.; Munger, J.W.; O’Keefe, J.; Schmid, H.P.; Wing, I.S. Net carbon uptake has increased through warming-induced changes in temperate forest phenology. *Nat. Clim. Chang.* **2014**, *4*, 598–604. [[CrossRef](#)]
31. Goetz, S.J.; Bunn, A.G.; Fiske, G.J.; Houghton, R. Satellite-observed photosynthetic trends across boreal North America associated with climate and fire disturbance. *Proc. Natl. Acad. Sci. USA* **2005**, *102*, 13521–13525. [[CrossRef](#)]
32. Verbesselt, J.; Hyndman, R.; Newnham, G.; Culvenor, D. Detecting trend and seasonal changes in satellite image time series. *Remote Sens. Environ.* **2010**, *114*, 106–115. [[CrossRef](#)]
33. Mildrexler, D.J.; Zhao, M.; Heinsch, F.A.; Running, S.W. A new satellite-based methodology for continental-scale disturbance detection. *Ecol. Appl.* **2007**, *17*, 235–250. [[CrossRef](#)]
34. Mildrexler, D.J.; Zhao, M.; Running, S.W. Testing a MODIS Global Disturbance Index across North America. *Remote Sens. Environ.* **2009**, *113*, 2103–2117. [[CrossRef](#)]
35. Vermote, E.; Vermeulen, A. *Atmospheric Correction Algorithm: Spectral Reflectances (MOD09)*; Version 4; Department of Geography, University of Maryland: College Park, MD, USA, 1999.
36. Cohen, W.B.; Spies, T.A.; Alig, R.J.; Oetter, D.R.; Maiersperger, T.K.; Fiorella, M. Characterizing 23 Years (1972–1995) of Stand Replacement Disturbance in Western Oregon Forests with Landsat Imagery. *Ecosystems* **2002**, *5*, 122–137. [[CrossRef](#)]
37. Zhou, Y.; Xiao, X.; Wagle, P.; Bajgain, R.; Mahan, H.; Basara, J.B.; Dong, J.; Qin, Y.; Zhang, G.; Luo, Y.; et al. Examining the short-term impacts of diverse management practices on plant phenology and carbon fluxes of Old World bluestems pasture. *Agric. For. Meteorol.* **2017**, *237–238*, 60–70. [[CrossRef](#)]
38. Schubert, S.D.; Suarez, M.J.; Pegion, P.J.; Koster, R.D.; Bacmeister, J.T. On the cause of the 1930s Dust Bowl. *Science* **2004**, *303*, 1855–1859. [[CrossRef](#)]
39. Hoerling, M.; Eischeid, J.; Kumar, A.; Leung, R.; Mariotti, A.; Mo, K.; Schubert, S.; Seager, R. Causes and predictability of the 2012 Great Plains drought. *Bull. Am. Meteorol. Soc.* **2014**, *95*, 269–282. [[CrossRef](#)]
40. Gu, Y.; Hunt, E.; Wardlow, B.; Basara, J.B.; Brown, J.F.; Verdin, J.P. Evaluation of MODIS NDVI and NDWI for vegetation drought monitoring using Oklahoma Mesonet soil moisture data. *Geophys. Res. Lett.* **2008**, *35*, L22401. [[CrossRef](#)]
41. Gu, Y.; Brown, J.F.; Verdin, J.P.; Wardlow, B. A five-year analysis of MODIS NDVI and NDWI for grassland drought assessment over the central Great Plains of the United States. *Geophys. Res. Lett.* **2007**, *34*, L06407. [[CrossRef](#)]
42. Christian, J.; Christian, K.; Basara, J.B. Drought and pluvial dipole events within the great plains of the United States. *J. Appl. Meteorol. Climatol.* **2015**, *54*, 1886–1898. [[CrossRef](#)]
43. Basara, J.B.; Maybourn, J.N.; Peirano, C.M.; Tate, J.E.; Brown, P.J.; Hoey, J.D.; Smith, B.R. Drought and associated impacts in the Great Plains of the United States—A review. *Int. J. Geosci.* **2013**, *4*, 72. [[CrossRef](#)]
44. Zhou, Y.; Xiao, X.; Zhang, G.; Wagle, P.; Bajgain, R.; Dong, J.; Jin, C.; Basara, J.B.; Anderson, M.C.; Hain, C.; et al. Quantifying agricultural drought in tallgrass prairie region in the U.S. Southern Great Plains through analysis of a water-related vegetation index from MODIS images. *Agric. For. Meteorol.* **2017**, *246*, 111–122. [[CrossRef](#)]
45. Brockway, D.G.; Gatewood, R.G.; Paris, R.B. Restoring fire as an ecological process in shortgrass prairie ecosystems: Initial effects of prescribed burning during the dormant and growing seasons. *J. Environ. Manag.* **2002**, *65*, 135–152. [[CrossRef](#)] [[PubMed](#)]
46. Twidwell, D.; Rogers, W.E.; Fuhlendorf, S.D.; Wonkka, C.L.; Engle, D.M.; Weir, J.R.; Kreuter, U.P.; Taylor, C.A. The rising Great Plains fire campaign: Citizens’ response to woody plant encroachment. *Front. Ecol. Environ.* **2013**, *11*, e64–e71. [[CrossRef](#)]
47. Reinhart, K.O.; Dangi, S.R.; Vermeire, L.T. The effect of fire intensity, nutrients, soil microbes, and spatial distance on grassland productivity. *Plant Soil* **2016**, *409*, 203–216. [[CrossRef](#)]
48. Wagle, P.; Gowda, P.H.; Northup, B.K.; Starks, P.J.; Neel, J.P. Response of tallgrass prairie to management in the US Southern Great Plains: Site descriptions, management practices, and eddy covariance instrumentation for a long-term experiment. *Remote Sens.* **2019**, *11*, 1988. [[CrossRef](#)]
49. Campioli, M.; Vicca, S.; Luysaert, S.; Bilcke, J.; Ceschia, E.; Chapin, F., III; Ciais, P.; Fernández-Martínez, M.; Malhi, Y.; Obersteiner, M. Biomass production efficiency controlled by management in temperate and boreal ecosystems. *Nat. Geosci.* **2015**, *8*, 843–846. [[CrossRef](#)]
50. Wagle, P.; Xiao, X.; Torn, M.S.; Cook, D.R.; Matamala, R.; Fischer, M.L.; Jin, C.; Dong, J.; Biradar, C. Sensitivity of vegetation indices and gross primary production of tallgrass prairie to severe drought. *Remote Sens. Environ.* **2014**, *152*, 1–14. [[CrossRef](#)]

51. McPherson, R.A.; Fiebrich, C.A.; Crawford, K.C.; Kilby, J.R.; Grimsley, D.L.; Martinez, J.E.; Basara, J.B.; Illston, B.G.; Morris, D.A.; Kloesel, K.A. Statewide monitoring of the mesoscale environment: A technical update on the Oklahoma Mesonet. *J. Atmos. Ocean. Technol.* **2007**, *24*, 301–321. [[CrossRef](#)]
52. Bajgain, R.; Xiao, X.; Basara, J.B.; Wagle, P.; Zhou, Y.; Mahan, H.; Gowda, P.H.; McCarthy, H.R.; Northup, B.; Neel, J.P.S.; et al. Carbon dioxide and water vapor fluxes in winter wheat and tallgrass prairie in central Oklahoma. *Sci. Total Environ.* **2018**, *644*, 1511–1524. [[CrossRef](#)]
53. Zhou, Y.; Xiao, X.; Qin, Y.; Dong, J.; Zhang, G.; Kou, W.; Jin, C.; Wang, J.; Li, X. Mapping paddy rice planting area in rice-wetland coexistent areas through analysis of Landsat 8 OLI and MODIS images. *Int. J. Appl. Earth Obs. Geoinf.* **2016**, *46*, 1–12. [[CrossRef](#)]
54. Xiao, X.; Hollinger, D.; Aber, J.; Goltz, M.; Davidson, E.A.; Zhang, Q.; Moore, B. Satellite-based modeling of gross primary production in an evergreen needleleaf forest. *Remote Sens. Environ.* **2004**, *89*, 519–534. [[CrossRef](#)]
55. Bajgain, R.; Xiao, X.; Basara, J.; Doughty, R.; Wu, X.; Wagle, P.; Zhou, Y.; Gowda, P.; Steiner, J. Differential responses of native and managed prairie pastures to environmental variability and management practices. *Agric. For. Meteorol.* **2020**, *294*, 108137. [[CrossRef](#)]
56. Otkin, J.A.; Anderson, M.C.; Hain, C.; Svoboda, M.; Johnson, D.; Mueller, R.; Tadesse, T.; Wardlow, B.; Brown, J. Assessing the evolution of soil moisture and vegetation conditions during the 2012 United States flash drought. *Agric. For. Meteorol.* **2016**, *218*, 230–242. [[CrossRef](#)]
57. Rogiers, N.; Eugster, W.; Furger, M.; Siegwolf, R. Effect of land management on ecosystem carbon fluxes at a subalpine grassland site in the Swiss Alps. *Theor. Appl. Climatol.* **2005**, *80*, 187–203. [[CrossRef](#)]
58. Zeeman, M.J.; Hiller, R.; Gilgen, A.K.; Michna, P.; Plüss, P.; Buchmann, N.; Eugster, W. Management and climate impacts on net CO₂ fluxes and carbon budgets of three grasslands along an elevational gradient in Switzerland. *Agric. For. Meteorol.* **2010**, *150*, 519–530. [[CrossRef](#)]
59. Kennedy, R.E.; Andréfouët, S.; Cohen, W.B.; Gómez, C.; Griffiths, P.; Hais, M.; Healey, S.P.; Helmer, E.H.; Hostert, P.; Lyons, M.B.; et al. Bringing an ecological view of change to Landsat-based remote sensing. *Front. Ecol. Environ.* **2014**, *12*, 339–346. [[CrossRef](#)]
60. McDowell, N.G.; Coops, N.C.; Beck, P.S.A.; Chambers, J.Q.; Gangodagamage, C.; Hicke, J.A.; Huang, C.-Y.; Kennedy, R.; Krofcheck, D.J.; Litvak, M.; et al. Global satellite monitoring of climate-induced vegetation disturbances. *Trends Plant Sci.* **2015**, *20*, 114–123. [[CrossRef](#)]
61. Hansen, M.C.; Potapov, P.V.; Moore, R.; Hancher, M.; Turubanova, S.; Tyukavina, A.; Thau, D.; Stehman, S.; Goetz, S.; Loveland, T. High-resolution global maps of 21st-century forest cover change. *Science* **2013**, *342*, 850–853. [[CrossRef](#)]
62. Gorelick, N.; Hancher, M.; Dixon, M.; Ilyushchenko, S.; Thau, D.; Moore, R. Google Earth Engine: Planetary-scale geospatial analysis for everyone. *Remote Sens. Environ.* **2017**, *202*, 18–27. [[CrossRef](#)]
63. Robinson, N.P.; Allred, B.W.; Jones, M.O.; Moreno, A.; Kimball, J.S.; Naugle, D.E.; Erickson, T.A.; Richardson, A.D. A Dynamic Landsat Derived Normalized Difference Vegetation Index (NDVI) Product for the Conterminous United States. *Remote Sens.* **2017**, *9*, 863. [[CrossRef](#)]
64. Suyker, A.E.; Verma, S.B.; Burba, G.G. Interannual variability in net CO₂ exchange of a native tallgrass prairie. *Glob. Chang. Biol.* **2003**, *9*, 255–265. [[CrossRef](#)]
65. Fischer, M.L.; Torn, M.S.; Billesbach, D.P.; Doyle, G.; Northup, B.; Biraud, S.C. Carbon, water, and heat flux responses to experimental burning and drought in a tallgrass prairie. *Agric. For. Meteorol.* **2012**, *166–167*, 169–174. [[CrossRef](#)]
66. Wagle, P.; Kakani, V.G.; Gowda, P.H.; Xiao, X.; Northup, B.K.; Neel, J.P.; Starks, P.J.; Steiner, J.L.; Gunter, S.A. Dormant Season Vegetation Phenology and Eddy Fluxes in Native Tallgrass Prairies of the US Southern Plains. *Remote Sens.* **2022**, *14*, 2620. [[CrossRef](#)]
67. Flynn, K.C.; Zhou, Y.; Gowda, P.H.; Moffet, C.A.; Wagle, P.; Kakani, V.G. Burning and Climate Interactions Determine Impacts of Grazing on Tallgrass Prairie Systems. *Rangel. Ecol. Manag.* **2020**, *73*, 104–118. [[CrossRef](#)]
68. Running, S.W.; Baldocchi, D.D.; Turner, D.P.; Gower, S.T.; Bakwin, P.S.; Hibbard, K.A. A Global Terrestrial Monitoring Network Integrating Tower Fluxes, Flask Sampling, Ecosystem Modeling and EOS Satellite Data. *Remote Sens. Environ.* **1999**, *70*, 108–127. [[CrossRef](#)]
69. Zhou, Y.; Flynn, K.C.; Gowda, P.H.; Wagle, P.; Ma, S.; Kakani, V.G.; Steiner, J.L. The potential of active and passive remote sensing to detect frequent harvesting of alfalfa. *Int. J. Appl. Earth Obs. Geoinf.* **2021**, *104*, 102539. [[CrossRef](#)]

Disclaimer/Publisher’s Note: The statements, opinions and data contained in all publications are solely those of the individual author(s) and contributor(s) and not of MDPI and/or the editor(s). MDPI and/or the editor(s) disclaim responsibility for any injury to people or property resulting from any ideas, methods, instructions or products referred to in the content.